

Temperature dependence of rho- and a_1 -meson masses and mixing of vector and axial-vector correlators

Michael Urban,¹ Michael Buballa,^{2,3} and Jochen Wambach²

¹*Institut de Physique Nucléaire, F-91406 Orsay Cedex, France*

²*Institut für Kernphysik, Schlossgartenstr. 9, D-64289 Darmstadt, Germany*

³*Gesellschaft für Schwerionenforschung, Planckstr. 1, D-64291 Darmstadt, Germany*

(Dated: October 2, 2001)

Within a chiral model which provides a good description of the properties of ρ and a_1 mesons in vacuum, it is shown that, to order T^2 , the ρ - and a_1 -meson masses remain constant in the chiral limit, even if at tree level they are proportional to the chiral condensate, σ_0 . Numerically, the temperature dependence of the masses turns out to be small also for realistic parameter sets and high temperatures. The weak temperature dependence of the masses is consistent with the Eletsky-Ioffe mixing theorem, and traces of mixing effects can be seen in the spectral function of the vector correlator at finite temperature.

PACS numbers: 14.40.Cs,11.30.Rd

It is commonly believed that the enhancement of the dilepton spectrum in the invariant mass range around 400 MeV observed in heavy-ion experiments [1] is a consequence of medium modifications of the ρ -meson spectral function, i.e., more precisely, the spectral function of the vector-isovector current-current correlation function, in hot and dense matter. Most of the more “conventional” calculations find a strongly increasing ρ meson width (see Ref. [2] and references therein), but the more speculative hypothesis of a “dropping ρ mass” by Brown and Rho [3] is being discussed as a viable alternative [4]. The aim of the present study is to combine the phenomenology included in the more “conventional” calculations with the constraints imposed by chiral symmetry. As a first step, we have constructed in Ref. [5] a chiral model which gives a good description of the vector and axial-vector spectral functions in vacuum. The model is based on the linear σ model, which has been extended to incorporate the ρ meson and its chiral partner, the $a_1(1260)$, as elementary fields. In this letter we will discuss results from the application of this model to finite temperatures.

Within the model presented in Ref. [5] the vector meson masses at tree level are given by

$$m_\rho^2 = m_0^2 + h_2 \sigma_0^2, \quad m_{a_1}^2 = m_0^2 + (h_1 + h_2) \sigma_0^2, \quad (1)$$

where m_0 is the vector-meson mass parameter in the Lagrangian, h_1 and h_2 are coupling constants, and σ_0 is the expectation value of the scalar field σ at tree level. As shown in Ref. [5], the parameter m_0 can take any value below ≈ 400 MeV, in particular, $m_0 = 0$. Thus, if Eq. (1) were valid in general, i.e., not only at tree level, “Brown-Rho scaling” would emerge, i.e., the vector meson masses would go to zero at the chiral phase transition, where $\langle \sigma \rangle$ vanishes.

A good description of the experimentally measured vector and axial-vector spectral functions in vacuum [8] can be achieved by including the one-loop ρ and a_1 self-energies, which comprise the dominant decay channels

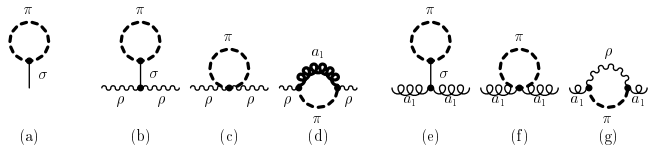


FIG. 1: Diagrams generating the dominant medium contributions to $\langle \sigma \rangle$ (a), Σ_ρ (b-d) and Σ_{a_1} (e-g).

$\rho \rightarrow \pi\pi$ and $a_1 \rightarrow \pi\rho$ as well as many other one-loop graphs which are necessary to comply with chiral symmetry [5]. The divergences generated by the loops can be canceled by chirally symmetric counterterms, which are adjusted such that masses at one loop are equal to those at tree level [5]. However, when we calculate the same diagrams at finite temperature T (i.e., when we replace the loop integrals over k_4 by a summation over discrete Matsubara frequencies $2\pi nT$), the masses at one loop become temperature dependent, while the masses at tree level remain constant.

Let us start by inspecting the temperature dependence of the condensate $\langle \sigma \rangle$. In the one-loop approximation it can be written as

$$\langle \sigma \rangle = \sigma_0 + \Delta\sigma_0, \quad (2)$$

where $\Delta\sigma_0$ denotes the sum of all one-loop tadpole graphs, divided by im_σ^2 [5]. It can be decomposed into vacuum and medium contributions, $\Delta\sigma_0 = \Delta\sigma_{0\,vac} + \Delta\sigma_{0\,med}$. The dominant medium contribution is generated by diagram (a) shown in Fig. 1. In the chiral limit, $m_\pi \rightarrow 0$, it is of the order T^2 , while all other one-loop diagrams are either vanishing ($\propto m_\pi^2$) or suppressed by $e^{-m/T}$, if the particle propagating in the loop has mass m . The explicit expression corresponding to diagram (a) reads

$$\Delta\sigma_{0\,med}^{(a)} = -\frac{3\sigma_0\lambda^2 Z_\pi}{2\pi^2 m_\sigma^2} \int_0^\infty d|\mathbf{k}| \mathbf{k}^2 \frac{n_\pi}{\omega_\pi}, \quad (3)$$

where the abbreviations $\omega_\pi = \sqrt{\mathbf{k}^2 + m_\pi^2}$ and $n_\pi = 1/(e^{\omega_\pi/T} - 1)$ have been used. The symbol λ denotes the usual coupling constant of the linear σ model, and $Z_\pi = Z_{\pi 1}$ is the residue of the pion propagator at tree level [5].

In the numerical calculations, the finite parts of the counterterms are determined such that f_π in vacuum remains unchanged by the loop corrections. In the chiral limit this has the consequence that $\Delta\sigma_{0\,vac}$ vanishes. Hence, we can replace σ_0 in Eq. (3) by $\langle\sigma\rangle_{T=0}$. For further simplification we make use of the relations $m_\sigma^2 = 2\lambda^2\sigma_0^2$ and $f_\pi = \sigma_0/\sqrt{Z_\pi}$, which follow from those given in Ref. [5] in the limit $m_\pi = 0$. In this way we finally obtain

$$\langle\sigma\rangle_{T\neq0} = \langle\sigma\rangle_{T=0} \left(1 - \frac{T^2}{8f_\pi^2} + \dots\right), \quad (4)$$

as required by chiral symmetry [9].

Let us now turn to the temperature dependence of the ρ self-energy $\Sigma_\rho(q_0, \mathbf{q})$, where q_0 and \mathbf{q} denote the energy and three-momentum of the ρ meson relative to the heat bath. In the following we will restrict ourselves to $\mathbf{q} = 0$. In this case the self-energy tensor $\Sigma_\rho^{\mu\nu}$ has, as in vacuum, only two independent components, namely the four-dimensionally longitudinal and transverse self-energies, Σ_ρ^l and Σ_ρ^t . In what follows we will concentrate on the latter and denote it by Σ_ρ for simplicity. Similar to $\Delta\sigma_0$, the self-energy Σ_ρ can be decomposed into vacuum and medium contributions. The dominant medium contributions are generated by the diagrams (b) to (d). The two-pion loop, which is the dominant graph in vacuum, does not contribute to order T^2 , because the pions couple to the ρ meson in p -wave, resulting in additional powers of the thermal pion momentum. The explicit expressions for the three contributions lead to

$$\Sigma_{\rho\,med}^{(b)} = 2h_2\sigma_0\Delta\sigma_{0\,med} \quad (5)$$

$$\Sigma_{\rho\,med}^{(c)} = \frac{(2h_1 + 3h_2)Z_\pi}{2\pi^2} \int_0^\infty d|\mathbf{k}| \mathbf{k}^2 \frac{n_\pi}{\omega_\pi}, \quad (6)$$

$$\begin{aligned} \Sigma_{\rho\,med}^{(d)} &= \frac{h_1^2\sigma_0^2Z_\pi}{2\pi^2} \int_0^\infty d|\mathbf{k}| \mathbf{k}^2 \frac{n_\pi}{\omega_\pi\omega_{a_1}} \\ &\times \left(\frac{\omega_{a_1} - \omega_\pi}{q_0^2 - (\omega_{a_1} - \omega_\pi)^2} + \frac{\omega_{a_1} + \omega_\pi}{q_0^2 - (\omega_{a_1} + \omega_\pi)^2} \right). \end{aligned} \quad (7)$$

(To obtain real and imaginary part, q_0 must be replaced by $q_0 + i\varepsilon$.) The contribution of diagram (d) takes a much simpler form in the chiral limit if, in addition, $T \ll |q_0 - m_{a_1}|$. In this case, to order T^2 , the pion momentum \mathbf{k} can be neglected in the second line of Eq. (7), i.e., $\omega_\pi = 0$ and $\omega_{a_1} = m_{a_1}$, and the sum of the three contributions reads

$$\Sigma_{\rho\,med}(q_0, 0) = \frac{T^2h_1\sigma_0^2}{6f_\pi^2} \frac{q_0^2 - m_\rho^2}{q_0^2 - m_{a_1}^2}. \quad (8)$$

The change of the ρ mass is governed by the real part of the self-energy at $q_0 \approx m_\rho$, but Eq. (8) implies in particular $\Sigma_{\rho\,med}(m_\rho, 0) = 0$. Thus, to order T^2 , the ρ mass does not change at all, even if the condensate decreases, because the self-energy contribution $\propto \Delta\sigma_{0\,med}$, diagram (b), is exactly canceled by the other diagrams, (c) and (d).

For the a_1 meson the situation is analogous. The dominant medium contributions to the a_1 self-energy are given by the diagrams (e) to (g). In exactly the same way as described above for Σ_ρ , one finds, to order T^2 :

$$\Sigma_{a_1\,med}(q_0, 0) = -\frac{T^2h_1\sigma_0^2}{6f_\pi^2} \frac{q_0^2 - m_{a_1}^2}{q_0^2 - m_\rho^2}. \quad (9)$$

This shows that also the a_1 mass remains constant. The fact that the ρ and a_1 masses do not change to order T^2 was already found within the so-called gauged linear σ model some time ago [10]. However, within the gauged linear σ model, this is less surprising, since the ρ mass is independent of σ_0 at tree level, and diagram (b) does not exist.

The results presented above are valid only in the chiral limit and at low temperatures. The more general case of $m_\pi \neq 0$ and higher temperatures can be analyzed numerically. Then, of course, not only the diagrams shown in Fig. 1, but all one-loop self-energy diagrams have to be included. We will use two different parameter sets: one of those listed in Ref. [5] (parameter set A), and one with a very small pion mass ($m_\pi = 0.1$ MeV) appropriate for the chiral limit. In both parameter sets we have chosen $m_0 = 0$, i.e., naively one would have expected "Brown-Rho scaling", as explained below Eq. (1).

As in Ref. [5], we define the one-loop corrected ρ mass $m_\rho^{(1)}$ as the position of the maximum of the ρ spectral function, rather than as the zero of the real part of the ρ propagator. This implies that $m_\rho^{(1)}$ could in principle change, even if $\Sigma_{\rho\,med}$ vanishes at $q_0 = m_\rho$. However, this subtlety does not change our conclusions for the low-temperature behavior of $m_\rho^{(1)}$ significantly, as can be seen in Fig. 2. In the chiral limit, $m_\rho^{(1)}$ stays almost constant at low T , whereas the condensate decreases rapidly according to Eq. (4). At very high temperatures ($T \gtrsim 150$ MeV), of course, the low-temperature expansion is no longer valid, and also the ρ mass starts to change. In the case $m_\pi = 140$ MeV, the main difference to the chiral limit is that all temperature effects are suppressed by $e^{-m_\pi/T}$, and therefore also the condensate remains almost constant below $T \approx 50$ MeV. At higher temperatures, the cancellation of the different contributions to $\Sigma_{\rho\,med}$ is not as perfect as in the chiral limit, resulting in a somewhat stronger temperature dependence of $m_\rho^{(1)}$ than in the case $m_\pi = 0$.

Our results corroborate earlier arguments [2] that in the chiral limit a change of the ρ or a_1 mass of the order T^2 would violate the Eletsky-Ioffe mixing theorem and

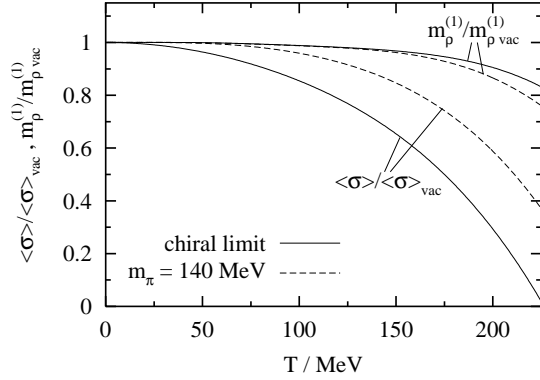


FIG. 2: The temperature dependence of the condensate $\langle\sigma\rangle$ and of the ρ mass $m_\rho^{(1)}$ in the chiral limit (solid lines) and for a realistic parameter set (dashed lines). All curves are normalized to their values at $T = 0$.

is therefore forbidden by chiral symmetry. This mixing theorem, which relies only on the current algebra of chiral symmetry, states that to order T^2 the vector and axial-vector current-current correlation functions $\Pi_V(q_0, \mathbf{q})$ and $\Pi_A(q_0, \mathbf{q})$, respectively, behave as follows [11]:

$$\Pi_V = (1 - \epsilon)\Pi_{V\,vac} + \epsilon\Pi_{A\,vac}, \quad (10)$$

$$\Pi_A = (1 - \epsilon)\Pi_{A\,vac} + \epsilon\Pi_{V\,vac}, \quad (11)$$

with $\epsilon = T^2/(6f_\pi^2)$.

It should be noted that the mixing coefficient ϵ is of order \hbar , since the mixing is generated by thermal pion loops. Hence, if the correlators are calculated in a strict loop expansion, the mixing theorem cannot be fulfilled exactly. E.g., if $\Pi_V^{(n)}$ and $\Pi_A^{(n)}$ denote the correlators to order \hbar^n (i.e., up to n loops), the medium contribution to $\Pi_V^{(1)}$ must be given by

$$\Pi_{V\,med}^{(1)} = \epsilon(\Pi_{A\,vac}^{(0)} - \Pi_{V\,vac}^{(0)}). \quad (12)$$

Since our Lagrangian is chirally symmetric, this relation is certainly fulfilled. At tree level the transverse parts of the correlators read

$$\Pi_V^{(0)}(q^2) = -\frac{(fq^2)^2}{q^2 - m_\rho^2}, \quad (13)$$

$$\Pi_A^{(0)}(q^2) = -\frac{(fq^2 - g\sigma_0^2)^2}{q^2 - m_{a_1}^2} - \sigma_0^2, \quad (14)$$

where f and g denote the $\gamma\rho$ and $\rho\pi\pi$ coupling constants, respectively [5]. The pion pole does not appear in Eq. (14), because it contributes only to the longitudinal part of the axial-vector correlator. The last term in Eq. (14) can be understood as the contribution of the $WW\sigma\sigma$ seagull vertex, if Π_A is computed via the W -boson self-energy. Next we turn to the left-hand side of Eq. (12), i.e., the medium contribution to $\Pi_V^{(1)}$. To order T^2 it

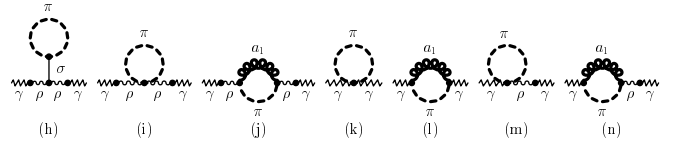


FIG. 3: Diagrams for the dominant medium contributions to Σ_γ in a strict loop expansion to one loop order.

is generated by the diagrams shown in Fig. 3. (As in Ref. [5], we draw diagrams for the photon self-energy $\Sigma_\gamma = -e^2\Pi_V$ rather than for Π_V .) The contribution of the diagrams (h) to (j) can be expressed in terms of the ρ self-energy:

$$\Pi_{V\,med}^{(1\,h-j)} = -\frac{(fq_0^2)^2}{(q_0^2 - m_\rho^2)^2} \Sigma_{\rho\,med}. \quad (15)$$

The diagrams (k) to (n), which can be evaluated with the same techniques as described for $\Sigma_{\rho\,med}$, give

$$\Pi_{V\,med}^{(1\,k)} = -\frac{T^2\sigma_0^2}{6f_\pi^2}, \quad (16)$$

$$\Pi_{V\,med}^{(1\,l)} = -\frac{T^2g^2\sigma_0^4}{6f_\pi^2} \frac{1}{q_0^2 - m_{a_1}^2}, \quad (17)$$

$$\Pi_{V\,med}^{(1\,m)} = \frac{T^2g\sigma_0^2fq_0^2}{6f_\pi^2} \frac{1}{q_0^2 - m_\rho^2}, \quad (18)$$

$$\Pi_{V\,med}^{(1\,n)} = \frac{T^2g\sigma_0^2fq_0^2}{6f_\pi^2} \frac{h_1\sigma_0^2}{(q_0^2 - m_{a_1}^2)(q_0^2 - m_\rho^2)}, \quad (19)$$

and the sum of all contributions reads

$$\begin{aligned} \Pi_{V\,med} &= \Pi_{V\,med}^{(1\,h-l)} + 2\Pi_{V\,med}^{(1\,m-n)} \\ &= \frac{T^2}{6f_\pi^2} \left(\frac{(fq_0^2)^2}{q_0^2 - m_\rho^2} - \frac{(fq_0^2 - g\sigma_0^2)^2}{q_0^2 - m_{a_1}^2} - \sigma_0^2 \right), \end{aligned} \quad (20)$$

which is exactly the result expected from Eq. (12).

However, in the model for Π_V and Π_A we presented in Ref. [5], the correlators are not calculated in a strict one-loop approximation. Instead, the Dyson series is summed, allowing for a successful description of Π_V in vacuum, but mixing all orders of \hbar . Thus the dominant medium contributions to Π_V are given by diagrams similar to those shown in Fig. 3, but with all bare ρ propagators $1/(q^2 - m_\rho^2)$ replaced by dressed ones, $G_{\rho\,vac}(q^2) = 1/[q^2 - m_\rho^2 - \Sigma_{\rho\,vac}(q^2)]$, and all point-like $\gamma\rho$ vertices f replaced by loop-corrected ones, $F_{\gamma\rho\,vac}(q^2)$.

In this approximation one can see that, to order T^2 , the imaginary part of Π_V (i.e., the spectral function) decreases in the neighborhood of m_ρ , but exactly at m_ρ it remains constant, i.e., the strength of the ρ meson peak is reduced by reducing its width and not its height. In addition, similar to Eq. (20), a peak $\propto \delta(q_0^2 - m_{a_1}^2)$ is generated, but the coefficient is different from that in Eq. (20). For demonstration, we have computed $\text{Im}\Pi_V$

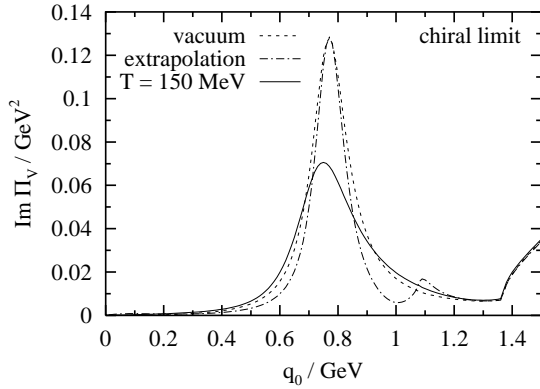


FIG. 4: The imaginary part of vector correlator, $\text{Im } \Pi_V(q_0, 0)$, in the chiral limit as function of energy, in vacuum (dashed line), as an extrapolation of the low-temperature behavior calculated for $T = 25$ MeV to $T = 150$ MeV (dash-dotted line), and at $T = 150$ MeV (solid line).

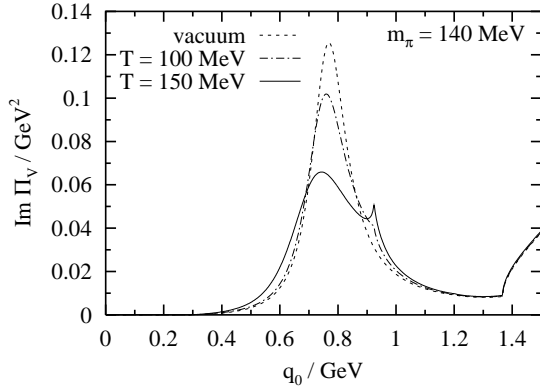


FIG. 5: The imaginary part of vector correlator, $\text{Im } \Pi_V(q_0, 0)$, for a realistic parameter set as function of energy, at various temperatures: $T = 0$ (dashed line), $T = 100$ MeV (dash-dotted line), and $T = 150$ MeV (solid line).

at $T = 25$ MeV and extrapolated the medium contribution to $T = 150$ MeV as if there were no effects beyond order T^2 . The result can be seen in Fig. 4 together with $\text{Im } \Pi_V^{\text{vac}}$. The third curve in Fig. 4 shows $\text{Im } \Pi_V$ calculated at $T = 150$ MeV. Obviously this looks completely different from the extrapolation of the low-temperature behavior. The peak at $q_0 = m_{a_1}$ is washed out by the thermal motion of the pions, which is so strong that the πa_1 loop [diagram (d)] generates an imaginary part not only at $q_0 \approx m_{a_1}$, but also at $q_0 \approx m_\rho$. Another important contribution is given by the two-pion loop, although it is of the order T^4 as discussed before Eq. (5). These two effects are the reasons for the broadening of the ρ -meson peak visible in Fig. 4.

To conclude this letter, we display in Fig. 5 some results for the vector correlator obtained with the realistic parameter set, i.e., $m_\pi = 140$ MeV. In this case, of course, the mixing in the form of Eq. (11) cannot occur,

since all temperature effects are suppressed by $e^{-m_\pi/T}$, and the axial correlator mixed into the vector correlator at energy q_0 must be taken at energies below $q_0 - m_\pi$ or above $q_0 + m_\pi$. Indeed, with increasing temperature, in addition to the broadening of the ρ -meson peak, a sharp peak at $q_0 = m_{a_1} - m_\pi$ shows up in $\text{Im } \Pi_V$, which can be interpreted in this sense. Unlike the peak at $q_0 = m_{a_1}$ in the chiral limit, this peak is not smeared by the thermal motion of the pions, because it results from a kink in Σ_ρ at the threshold $q_0 = m_{a_1} - m_\pi$, which persists to arbitrary temperatures. The existence of this threshold, and therefore of the peak in $\text{Im } \Pi_V$, is of course an artifact of our approximation, in which the a_1 -mesons inside the loops have no width. In a more realistic model this reminiscence of the Eletsky-Ioffe mixing would reduce to a smooth enhancement of $\text{Im } \Pi_V$ above the ρ -meson peak. In order to see this, an approximation scheme, in which also the particles inside the loops are dressed self-consistently, is desirable [12].

In order to draw quantitative conclusions for observables which are directly accessible by heavy-ion experiments (e.g., dilepton rates), also the effects of finite three-momentum \mathbf{q} , and, more importantly, of finite baryon density, must be included. The former is straightforward, but the inclusion of baryonic effects in a chirally symmetric way is a very difficult task and is postponed to future work.

One of us (MU) acknowledges support from the Alexander von Humboldt foundation and would like to thank Prof. G. Chanfray for the hospitality at the IPN Lyon. This work was supported in part by the BMBF.

- [1] G. Agakichiev *et al.* (CERES collaboration), Phys. Rev. Lett. **75**, 1272 (1995); P. Wurm for the CERES collaboration, Nucl. Phys. **A590**, 103c (1995).
- [2] R. Rapp and J. Wambach, Adv. Nucl. Phys. **25**, 1 (2000).
- [3] G.E. Brown and M. Rho, Phys. Rev. Lett. **66**, 2720 (1991).
- [4] G.E. Brown and M. Rho, nucl-th/0101015.
- [5] M. Urban, M. Buballa, and J. Wambach, hep-ph/0102260.
- [6] C.D. Froggatt and J.L. Petersen, Nucl. Phys. **B129**, 89 (1977).
- [7] S.R. Amendolia *et al.*, Phys. Lett. B **138**, 454 (1984); **146**, 116 (1984).
- [8] R. Barate *et al.* (ALEPH Collaboration), Eur. Phys. J. C **4**, 409 (1998).
- [9] J. Gasser and H. Leutwyler, Phys. Lett. B **184**, 83 (1987).
- [10] R.D. Pisarski, hep-ph/9505257; Phys. Rev. D **52**, R3773 (1995).
- [11] M. Dey, V.L. Eletsy, and B.L. Ioffe, Phys. Lett. B **252**, 620 (1990); V.L. Eletsy and B.L. Ioffe, Phys. Rev. D **51**, 2371 (1995).
- [12] H. van Hees and J. Knoll, Nucl. Phys. **A683**, 369 (2000).